

# Thermodynamic and optical properties of mixed-salt aerosols of atmospheric importance

Ignatius N. Tang

Environmental Chemistry Division, Department of Applied Science, Brookhaven National Laboratory, Upton, New York

**Abstract.** Extensive water activity, density, and refractive index data at 25°C are reported for mixed-salt solutions, NaCl-KCl, NaCl-NaNO<sub>3</sub>, NaCl-Na<sub>2</sub>SO<sub>4</sub>, Na<sub>2</sub>SO<sub>4</sub>-NaNO<sub>3</sub>, and (NH<sub>4</sub>)<sub>2</sub>SO<sub>4</sub>-Na<sub>2</sub>SO<sub>4</sub>. The data are obtained from hydration experiments using the single-particle levitation technique developed recently for measuring the thermodynamic and optical properties of microdroplets. These data, covering the whole concentration range from dilute solutions to high supersaturations, provide an opportunity to explore the light-scattering properties of both internal and external mixtures of the chloride, sulfate, and nitrate aerosols of atmospheric importance. It is shown that for sulfate and nitrate aerosols as solution droplets, the light-scattering properties do not differ appreciably among all mixture types and compositions, as long as the dry-salt aerosols have the same particle-size distribution. However, for mixed-salt aerosols containing NaCl, the light-scattering properties do depend upon the composition and particle-size distribution, although not so much on the mixture type.

## Introduction

It is well known that atmospheric aerosols not only play a dominant role in determining the local air quality and visibility impairment [Seinfeld, 1989; Sloane and White, 1986] but also contribute substantially to radiative forcing in the opposite direction of the greenhouse gases [Charlson *et al.*, 1992]. The chemical composition of atmospheric aerosols is highly complex and often varies with time and location. Frequently, however, the ambient aerosol contains large portions of inorganic salts such as sulfates, nitrates, and chlorides in either pure or mixed forms. These salt aerosols are hygroscopic by nature and exhibit the property of deliquescence when the relative humidity (RH) increases. Once in solution, a saline droplet will continue to grow by water vapor condensation as RH further increases. Conversely, as RH decreases, the droplet will evaporate and remain in a metastable liquid solution supersaturated with the salt before crystallization finally takes place [Orr *et al.*, 1958; Tang, 1980; Rood *et al.*, 1989]. Consequently, extensive water activity and density data as a function of solute concentration are required in droplet growth and evaporation computations for aerosols under changing RH conditions. In addition, droplet light-scattering calculations require refractive index data as a function of chemical composition [Tang *et al.*, 1981; Sloane, 1983; Larson *et al.*, 1988].

Thermodynamic and optical properties of aqueous solution droplets containing a single salt of either sulfate or nitrate over extended concentrations have recently been reported [Tang and Munkelwitz, 1994a]. These data have been incorporated into a visibility model for computing light-scattering by hygroscopic aerosols as a function of RH [Tang, 1996]. It is shown that for a given size distribution, the extent of light scattered by aerosol

particles per unit dry-salt mass concentration is only weakly dependent on the chemical constituents of the hygroscopic sulfate and nitrate aerosols. Sulfuric acid and sodium chloride aerosols are exceptions and scatter light more efficiently than all other inorganic salt aerosols considered in the study. It is also shown that, based on limited mixed-salt data, both internal and external mixtures of the (NH<sub>4</sub>)<sub>2</sub>SO<sub>4</sub> and NH<sub>4</sub>NO<sub>3</sub> aerosols appear to exhibit similar light-scattering properties. Clearly, more data on mixed-salt systems are needed not only to ascertain the light-scattering properties but for use as input to relevant mathematical models describing the dynamic behavior and radiative effects of atmospheric aerosols.

In this paper, thermodynamic and optical properties at 25°C are presented for aqueous solution droplets containing ternary mixtures (two salts and water) of NaCl, KCl, Na<sub>2</sub>SO<sub>4</sub>, (NH<sub>4</sub>)<sub>2</sub>SO<sub>4</sub>, and NaNO<sub>3</sub> over extended concentrations. These data provide an opportunity to further explore the light-scattering properties of both internal and external mixtures of the chloride, sulfate, and nitrate aerosols of atmospheric importance.

## Experimental Procedure

The single-particle levitation technique employed in this study has been described elsewhere [Tang and Munkelwitz, 1994a]. Briefly, an electrostatically charged dry-salt particle, 6-8 μm in diameter, is trapped at the null point of an electrodynamic balance by an ac field imposed on a ring electrode surrounding the particle. The particle is balanced against gravity by a dc potential,  $U$ , established between two endcap electrodes positioned symmetrically above and below the particle. All electrode surfaces are hyperboloidal in shape and separated by Teflon insulators. When balanced at the null point, the particle mass  $w$  is given by

$$w = \frac{qU}{gZ_0} \quad (1)$$

where  $q$  is the number of electrostatic charges carried by the

This paper is not subject to U.S. Copyright. Published in 1997 by American Geophysical Union.

Paper number 96JD03085.

particle,  $g$  is the gravitational constant, and  $Z_0$  is the characteristic dimension of the cell. A vertically polarized He-Ne laser is used to illuminate the particle. The particle position is continuously monitored by a CCD video camera and displayed on a TV screen for precise null point balance. The 90° scattered light is also continuously monitored with a photomultiplier tube.

Initially, a filtered solution of known composition is loaded in a particle gun; a charged particle is injected into the cell and captured in dry  $N_2$  at the center of the cell by properly manipulating the ac and dc voltages applied to the electrodes. The system is closed and evacuated to a pressure below  $10^{-7}$  torr. The vacuum is then valved off, and the dc voltage required to position the particle at the null point is now noted as  $U_0$ . The system is then slowly back-filled with water vapor during particle deliquescence and growth. Conversely, the system is gradually evacuated during droplet evaporation and efflorescence. The water vapor pressure  $p$  and the balancing dc voltage  $U$  are simultaneously recorded in pairs. Thus the ratio  $U_0/U$  represents the solute mass fraction  $w_0/w$  and the ratio  $p/p^*$  represents the corresponding water activity  $a_w$  at that point. Here  $p^*$  is the saturation vapor pressure of water at the system temperature. The measurement can be repeated several times with the same particle by simply raising the water vapor pressure again and repeating the cycle. The reproducibility is better than  $\pm 2\%$ .

In order to establish the mixing rules for the density and refractive index of mixed-salt solutions, separate experiments were carried out to obtain the necessary aqueous solution data. Thus density measurements for bulk solutions were made using glass pycnometers, the volumes of which were calibrated with mercury at specific temperatures. Refractive index measurements were made with a Bausch and Lomb Abbe-31 refractometer equipped with a circulating thermostat.

## Results and Discussion

**Phase transformation and water activity.** Hygroscopic aerosol particles undergo the processes of phase transformation, droplet growth, and evaporation when the ambient RH is changing. The hydration behavior of a mixed-salt particle is more complicated in that after it has first deliquesced, it may then go through partially dissolved states before finally becoming a homogeneous solution droplet [Tang, 1976; Tang *et al.*, 1978]. This is illustrated in Figure 1 by the growth (shown as crosses) of a mixed-salt particle composed of equal molar NaCl and  $Na_2SO_4$ . The particle is observed to deliquesce at 74.2% RH, followed by a region where excess  $Na_2SO_4$  gradually dissolves in the solution as RH increases. Here, percent RH is defined as  $100p/p^*$ , or  $100a_w$ . The particle becomes a homogeneous solution droplet at about 80% RH and grows continuously and smoothly in the undersaturated region as RH increases further. The droplet growth measurement is seen to blend in very well with the isopiestic data (shown as filled squares) available in the literature for low concentrations [Platford, 1968]. As RH decreases (shown as open circles), the solution droplet is also observed to evaporate and become highly supersaturated until it crystallizes at about 53% RH. The hydration behavior shown in Figure 1 is typical of mixed-salt aerosols [Tang and Munkelwitz, 1993, 1994b]. For comparison, the hydration behavior of single-salt aerosol particles is also illustrated in Figure 1 for the components NaCl and  $Na_2SO_4$ ,

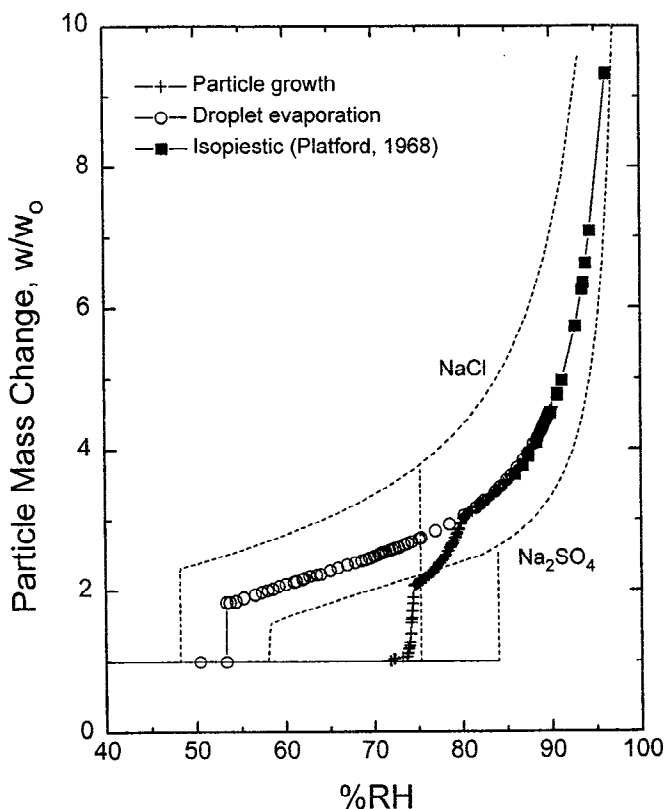


**Figure 1.** Phase transformation, growth, and evaporation of a mixed NaCl- $Na_2SO_4$  particle as a function of relative humidity.

shown as the dashed curves. Note that, although the decahydrate,  $Na_2SO_4 \cdot 10H_2O$ , is the stable solid in equilibrium with the saturated solution at room temperature, a supersaturated solution droplet under ambient conditions rarely crystallizes to form the decahydrate [Cohen *et al.*, 1987; Tang and Munkelwitz, 1994a], which if formed would then deliquesce at 93% RH. Instead, it crystallizes into an anhydrous particle, which deliquesces at 84% RH as shown. The mixed-salt particles containing  $Na_2SO_4$  are also not observed to form hydrates.

Thus droplet evaporation measurements provide a source of water activity data for single- and mixed-salt solutions over a large concentration range, especially in the highly supersaturated region where isopiestic measurements with bulk solutions are not accessible. For single-salt solutions, the water activity data may be fitted with simple polynomial expressions in either molality [Teng and Lenzi, 1974] or solute wt% [Tang and Munkelwitz, 1994a], although there are semiempirical expressions extending the Debye-Hückel limiting law to moderate concentrations [Hamer and Wu, 1972; Bromley, 1973; Pitzer, 1973]. Various methods have been proposed for predicting thermodynamic properties of multicomponent solutions and some of these methods have been reviewed by Sanster and Lenzi [1974] and Saxena and Peterson [1981]. Recently, Clegg and Pitzer [1992], Clegg *et al.* [1992], and Clegg and Brimblecombe [1995] have extended a mole-fraction-based thermodynamic model, originally developed by Pitzer and Simonson [1986] for mixtures containing ions of symmetrical charge type, to mixtures containing ions of arbitrary types. The advanced models are usually quite complicated but do not necessarily offer distinct advantages over some simple empirical models in terms of prediction capability.

**Table 1.** Summary of Polynomial Coefficients for Water Activities and Densities

	(NH <sub>4</sub> ) <sub>2</sub> SO <sub>4</sub>	Na <sub>2</sub> SO <sub>4</sub>	NaNO <sub>3</sub>	NaCl	KCl
$a_w$	1-0.37	1-0.58	1-0.3	1-0.47	1-0.62
$B_0$	110.65495	559.83158	310.21762	58.75248	135.02439
$B_1$	-367.59197	-2569.42664	-1829.75944	-187.81997	-475.35798
$B_2$	504.62934	4474.50201	5134.45395	272.11377	697.38495
$B_3$	-315.43839	-3450.21842	-8012.00018	-184.58287	-476.21938
$B_4$	67.70824	985.27913	7076.30664	41.53689	119.16158
$B_5$			-3333.65806		
$B_6$			654.42029		
$x, \%$	0-78	0-40	0-98	0-45	0-44
$A_1$	5.92(-3)*	8.871(-3)	6.521(-3)	7.41(-3)	6.13(-3)
$A_2$	-5.036(-6)	3.195(-5)	3.025(-5)	-3.741(-5)	4.53(-5)
$A_3$	1.024(-8)	2.28(-7)	1.437(-7)	2.252(-6)	-1.242(-6)
$A_4$				-2.06(-8)	1.582(-8)

\*Read 5.92(-3) as  $5.92 \times 10^{-3}$ .

In this work, the simple empirical relationship, known as the ZSR relation [Zdanovskii, 1936; Stokes and Robinson, 1966], is adopted as a means to express the water activity of mixed-salt solutions. For a semi-ideal ternary aqueous solution containing two electrolytes (designated 2 and 3) at a total molality  $m = m_2 + m_3$ , the ZSR relation,

$$\frac{1}{m} = \frac{z_2}{m_{02}} + \frac{z_3}{m_{03}} \quad (2)$$

holds when the solution is in isopiestic equilibrium (i.e., at same  $a_w$ ) with the binary solutions of the individual electrolytes at respective molalities  $m_{02}$  and  $m_{03}$ . Here  $z_2 = m_2/m$  and  $z_3 = m_3/m$  are mole fractions of the dry solutes. Semi-ideality refers to the case where the two solutes may interact with the solvent but not with each other. Systems showing departure from semi-ideality are common [Sanster and Lenzi, 1974]. For such systems, a third term,  $bz_2z_3$ , may be added to the right-hand side of equation (2), where  $b$  is an empirically determined parameter for each system. In this work, it is found that water activity data are conveniently represented by taking  $b$  as a linear function of  $a_w$ , namely,

$$b = A + Ba_w \quad (3)$$

where  $A$  and  $B$  are constants determined by the best fit of water activity data for all compositions and concentrations. Such a representation has also been shown by other investigators [Kirginsev and Luk'yanov, 1966; Sanster et al., 1973] to hold for many aqueous solutions at low concentrations. The combination of equation (2) and (3) is the extended ZSR relation to be used throughout this work.

In order to use the extended ZSR relation, it is necessary to express the molality of the binary solution of any given single electrolyte,  $m_{0j}$ , as a function of water activity. The following polynomial expression is used:

$$m_{0j} = \sum B_i a_w^i \quad (4)$$

where  $B_i$  is the coefficient of the  $i$ th term in the polynomial expression representing the given electrolyte solution. Water activity data for the binary solutions relevant to this work have already been published [Tang et al., 1986; Tang and Munkelwitz,

1994a]. Table 1 is a list of the  $B_i$  values derived from the published data for these binary solutions.

Figure 2 shows a fit of the measured water activity data with the extended ZSR relation for the mixed-salt NaCl-Na<sub>2</sub>SO<sub>4</sub> system. The data points were taken from isopiestic measurements [Platford, 1968] and droplet evaporation measurements that have already been shown in Figure 1. The solid curve is the best fit line calculated from the single-salt data given in Table 1, yielding  $A = 0.065$  and  $B = -0.036$ . The average error, percent error, is measured by the percent deviation of the calculated molality,  $m(\text{calc})$ , from the measured

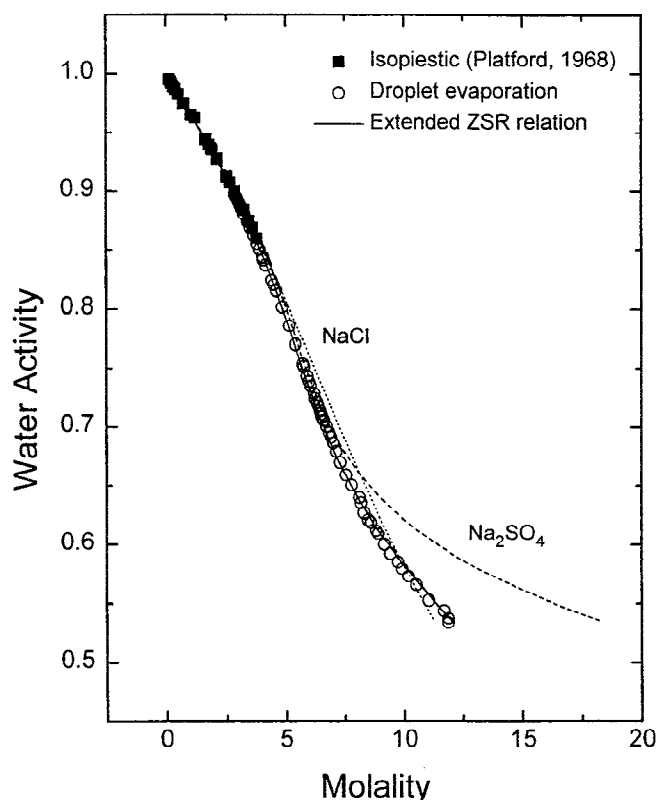


**Figure 2.** Experimental and ZSR-predicted water activities as a function of solution molality for the mixed-salt system: NaCl-Na<sub>2</sub>SO<sub>4</sub>-H<sub>2</sub>O.

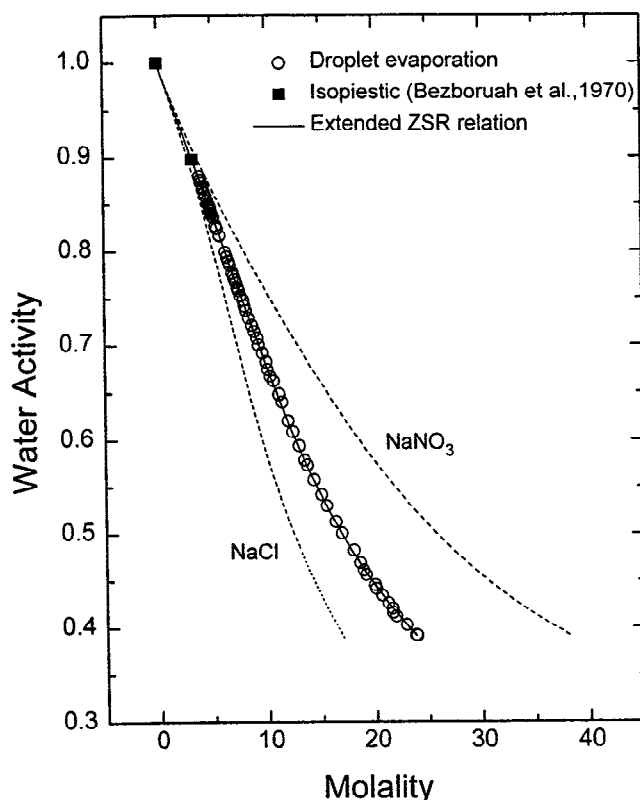


Figure 3. Experimental and ZSR-predicted water activities as a function of solution molality for the mixed-salt system: NaCl-NaNO<sub>3</sub>-H<sub>2</sub>O.

molality,  $m(\text{expl})$ , averaged over all measured water activities, namely,

$$\text{percent error} = \frac{100}{N} \sum \frac{|m(\text{expl})_i - m(\text{calc})_i|}{m(\text{expl})_i} \quad (5)$$

where  $N$  is the number of experimental points. In the present case, the average error in molality is 1.38% for the NaCl-Na<sub>2</sub>SO<sub>4</sub> system. Note that in Figure 2, the water activity data as a function of solution molality are also plotted for the single salts for comparison with the mixed salt. It happens that for some pairs of single salts the water activity data, when plotted as a function of molality, result in two curves which stay close together and even cross each other in some regions. The same data, however, when plotted as a function of mass concentration, become separated at all concentrations as clearly shown in Figure 1.

As a contrast to the NaCl-Na<sub>2</sub>SO<sub>4</sub> system, the evaporation data for an equal molar NaCl-NaNO<sub>3</sub> solution droplet are presented as the open symbols in Figure 3, together with the single-salt data shown as the dashed curves, which are well separated from each other in this case. There are published isopiestic measurements for mixed-salt solutions [Bezboruah *et al.*, 1970], which cover several compositions ranging from 0.2433 to 0.8599 mole fraction Na<sub>2</sub>SO<sub>4</sub>. Two such measurements for an equal molar solution are shown in Figure 3 as the solid squares. Since in principle the parameters  $A$  and  $B$  in equation (3) are independent of composition, available literature data of all compositions were therefore combined with the droplet evaporation data for evaluating  $A$  and  $B$ . The best fit, as shown by the solid curve in Figure 3, gives  $A=0.008$  and

$B=0.015$ . It is clear from the plot that the droplet evaporation data, which cover an extended concentration range, are consistent with the limited literature data for bulk solutions at low concentrations. The average error in molality is only 0.59% for the NaCl-NaNO<sub>3</sub> system. Note that, as indicated in Table 1, the water activity data for NaCl are only valid in the range 1-0.47. In this case, however, an extrapolation of the data down to 0.38 is necessary because of the fact that mixed-salt solution droplets tend to persist in the metastable state to this lower water activity. This fact is depicted in Figure 3, where the dotted line at the end of the NaCl curve is the extrapolation. Judging by the good fit shown for the mixed-salt system over the entire concentration range, it is concluded that the extrapolation is reasonable and justified.

The water activity data for the Na<sub>2</sub>SO<sub>4</sub>-NaNO<sub>3</sub> system are presented in Figure 4. The dashed curves represent the single-salt data as indicated, whereas the points are droplet evaporation measurements for mixed salts of four different compositions. The water activities in these measurements range from 0.84 to 0.49. Since for Na<sub>2</sub>SO<sub>4</sub>, the water activity data given in Table 1 are only valid in the range 1-0.58, an extrapolation to 0.49 is necessary in order to use the extended ZSR relation. The extrapolated data are shown in Figure 4 as the dotted curve continuing from the Na<sub>2</sub>SO<sub>4</sub> curve. The extended ZSR predictions for mixed salts are shown as the solid curves for each composition, using  $A=0.15$  and  $B=-0.064$  to produce the best fit for all data points. The average error in molality is 1.81%.

A further example showing that parameters  $A$  and  $B$  in equation (3) are indeed independent of composition is provided by the mixed-salt system NaCl-KCl. The isopiestic

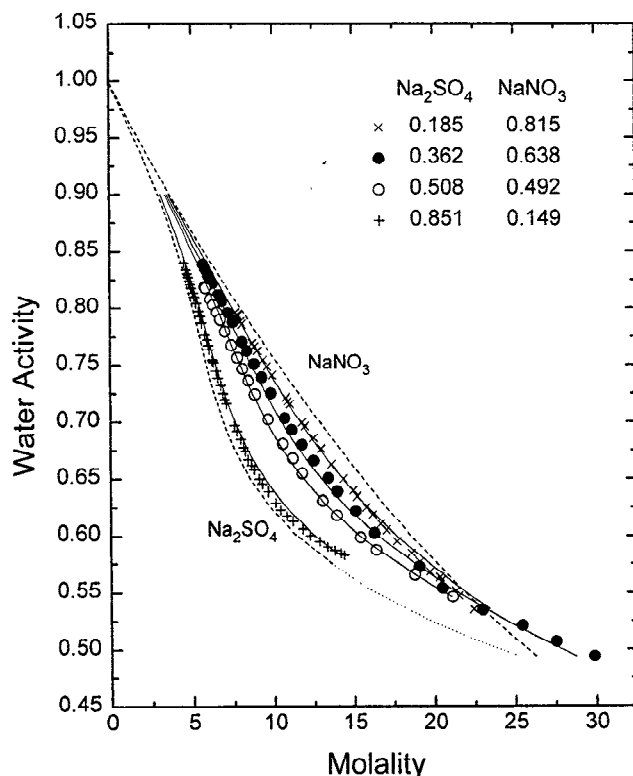


Figure 4. Experimental and ZSR-predicted water activities as a function of solution molality for the mixed-salt system: Na<sub>2</sub>SO<sub>4</sub>-NaNO<sub>3</sub>-H<sub>2</sub>O.

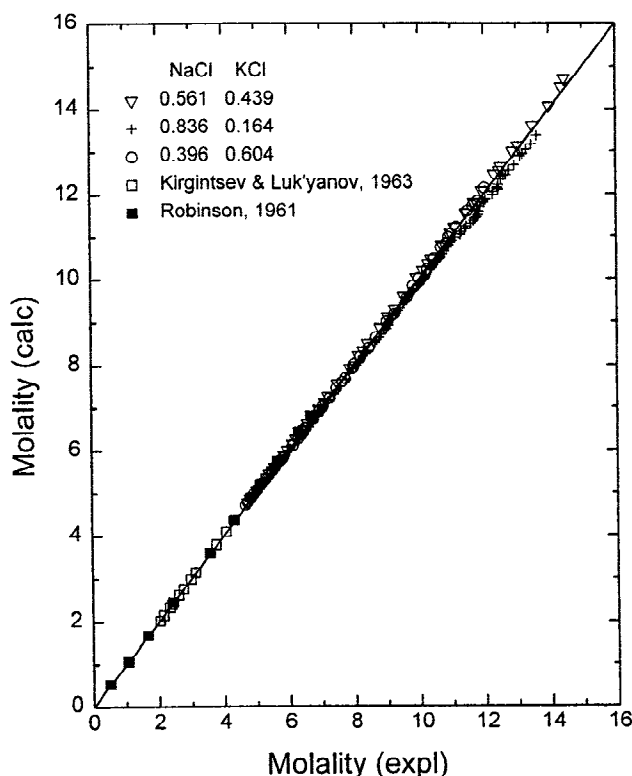


Figure 5. Comparison between experimental and ZSR-predicted molalities for the mixed-salt system: NaCl-KCl-H<sub>2</sub>O, at various molar compositions.

measurements for bulk solutions have been reported by Robinson [1961] in the water activity range between 0.984 and 0.760 and by Kirgintsev and Luk'yanov [1963] between 0.931 and 0.852, covering various compositions. Our droplet evaporation measurements also cover the range between 0.84 and 0.50 for three different compositions. Figure 5 is a plot of predicted molality,  $m(\text{calc})$ , versus measured molality,  $m(\text{expl})$ , for all data points mentioned above, yielding  $A=0.014$  and  $B=-0.045$  for the best fit. The average error in molality is 0.95%. The results indicate that for the NaCl-KCl system, the droplet evaporation data nicely extend the isopiestic data from the undersaturated region into the highly supersaturated region and that the extended ZSR relation is a good representation of the water activity data for all concentrations.

Water activity data for the  $(\text{NH}_4)_2\text{SO}_4$ - $\text{Na}_2\text{SO}_4$  system were also obtained. In Figure 6, the data are presented for four different compositions as indicated. Note that at molalities greater than about 14, it is necessary to extrapolate the  $\text{Na}_2\text{SO}_4$  water activity to 0.4. In the present case, the extended ZSR relation with a constant parameter,  $b=0.025$ , was found to represent the best fit for all droplet compositions investigated. The average error in molality is 2.3%.

**Density and partial molal refraction.** In an experiment, the intensity of light scattered from an evaporating droplet is continuously monitored at the 90° angle to the incident laser beam. A typical light-scattering diagram obtained for an aqueous  $(\text{NH}_4)_2\text{SO}_4$  droplet is shown in Figure 7a, revealing minute details of the Mie scattering resonances. As water evaporates from the droplet, the nonvolatile solute becomes increasingly concentrated. As a result, both the density and refractive index of the solution droplet are changing with the

droplet concentration. At the end of the experiment, the droplet reaches the critical supersaturation and suddenly transforms into a solid particle. The transition is unmistakably identified not only by a sudden drop in the dc voltage but also by the noisy light-scattering pattern characteristic of a solid particle.

Since the solute concentration in an evaporating droplet is known at any time from the dc measurement, it is possible to deduce the density and refractive index simultaneously from the droplet light-scattering diagram by Mie theory. The computational method has been described elsewhere [Tang and Munkelwitz, 1991]. It has also been shown previously [Tang and Munkelwitz, 1991, 1994a] that the partial molal refraction approach proposed by Stelson [1990] for undersaturated electrolyte solutions is equally applicable to supersaturated binary solutions, as investigated by the droplet evaporation method. In the present work, the study is extended to cover the aqueous solutions of mixed salts over the entire concentration range.

By definition, the molal refraction of either a pure substance or a homogenous mixture of molal volume  $V$  and refractive index  $n$  is given by Moelwyn-Hughes [1961]:

$$R = \frac{V(n^2 - 1)}{(n^2 + 2)} \quad (6)$$

For a ternary solution of solvent mole fraction  $y_1$  and solute mole fractions  $y_2$  and  $y_3$ , the molal refraction may be expressed as the sum of partial molal refraction of the solvent  $R_1$  and solutes  $R_2$  and  $R_3$  as follows:

$$R = y_1 R_1 + y_2 R_2 + y_3 R_3 \quad (7)$$

and the molal volume in equation (6) is given by:

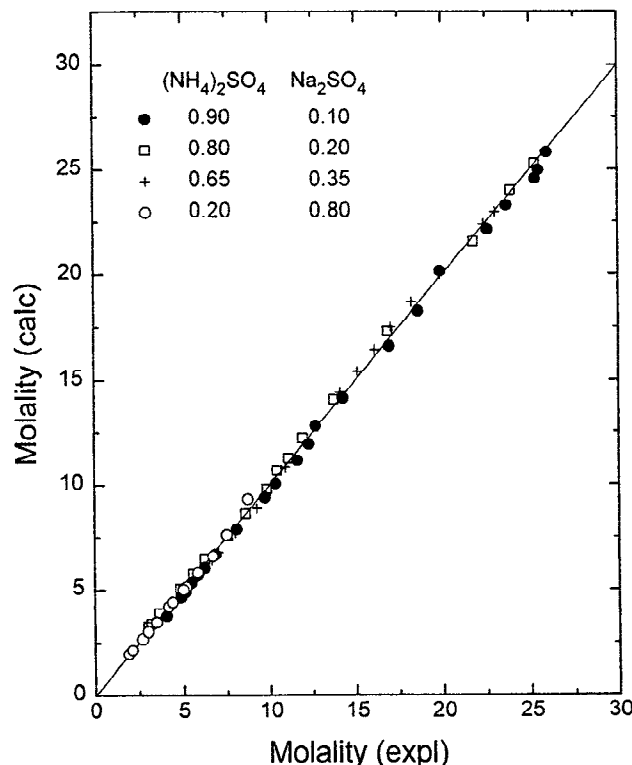
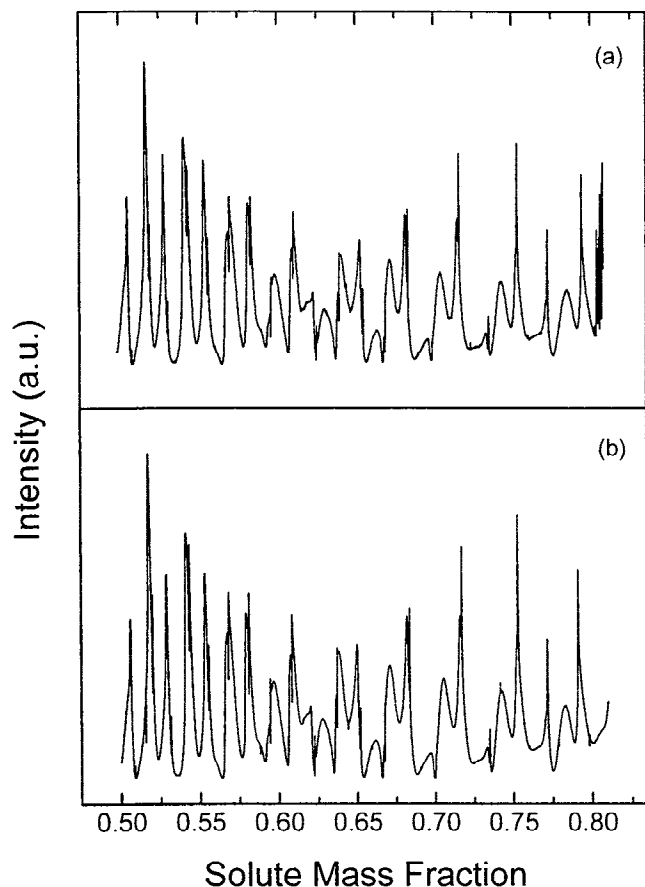


Figure 6. Comparison between experimental and ZSR-predicted molalities for the mixed-salt system:  $(\text{NH}_4)_2\text{SO}_4$ - $\text{Na}_2\text{SO}_4$ -H<sub>2</sub>O at various molar compositions.



**Figure 7.** Light-scattering diagram of an evaporating  $(\text{NH}_4)_2\text{SO}_4$  solution droplet (a.u., arbitrary units): (a) measurement and (b) computation.

$$V = \frac{1}{d} (y_1 M_1 + y_2 M_2 + y_3 M_3) \quad (8)$$

where  $d$  is the density of the solution and  $M_1$ ,  $M_2$  and  $M_3$  are the molecular weights of the solvent and solutes, respectively.

The partial molal refraction of a solute is the sum of the partial ionic refractions of all ions composing the solute molecule. Table 2 lists the partial ionic refractions of some common ions. These values have been validated for all concentrations, using the droplet evaporation method.  $R_1$  is taken as 3.717 for water. The density of a binary solution is expressed by the polynomial

$$d_{0j} = 0.9971 + \sum A_i x^i \quad (9)$$

where  $x$  is wt% of the solute and  $A_i$  is the coefficient of the  $i$ th term. The coefficients have been determined for the electrolyte solutions relevant to this study [Tang and Munkelwitz, 1994a; Tang, 1996], using the droplet evaporation technique. For convenience, these coefficients are given again in Table 1. There are several combination rules proposed for predicting the density of a multicomponent solution from binary data [Teng and Lenzi, 1975; Teng et al., 1976]. However, the following simple volume additivity rule is found to be adequate for most of the systems studied in this work:

$$\frac{1}{d} = \frac{x_2}{d_{02}} + \frac{x_3}{d_{03}} \quad (10)$$

**Table 2.** Partial Ionic Refractions of Electrolytic Ions in Aqueous Solutions

Ion	Value
$\text{H}^+$	0
$\text{Na}^+$	0.86
$\text{K}^+$	3.21
$\text{NH}_4^+$	5.01
$\text{Mg}^{++}$	0.03
$\text{Cl}^-$	8.09
$\text{NO}_3^-$	10.36
$\text{SO}_4^{=}, \text{HSO}_4^-$	13.44

where  $d_{02}$  and  $d_{03}$  are densities of binary solutions at the total solute concentration  $x$  of the mixed-salt solution. The mass fractions of the dry solutes are  $x_2$  and  $x_3$ , respectively. Thus, if the solution contains  $w_1$  grams of water and  $w_2$ , and  $w_3$  grams of salts 2 and 3, respectively, then, by definition,  $x = 100(w_2 + w_3)/(w_1 + w_2 + w_3)$ ,  $x_2 = w_2/(w_2 + w_3)$ , and  $x_3 = 1 - x_2$ .

Twenty-nine ternary solutions were prepared from the salts  $\text{NaCl}$ ,  $\text{Na}_2\text{SO}_4$ ,  $\text{NaNO}_3$ ,  $\text{MgSO}_4$ , and  $\text{MgCl}_2$ . The concentrations ranged between 15 and 37% by weight. The density and refractive index of each solution were determined at 25°C. In Figure 8, densities calculated by equation (10) for these solutions are plotted versus the measured values. The average error in density is only 0.12%. The open symbols are some limited literature data, mostly at low concentrations. In Figure 9, refractive indices calculated by the partial molal

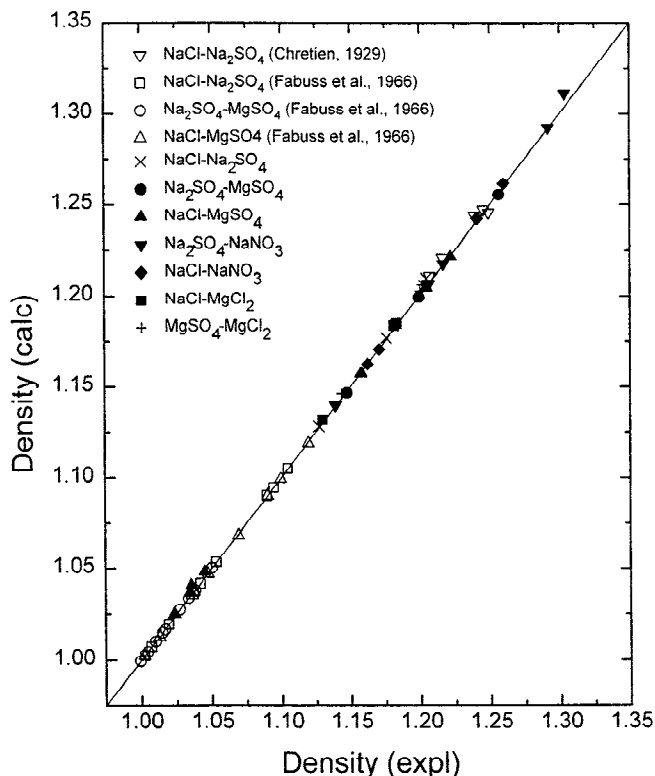


**Figure 8.** Comparison between experimental and predicted densities of various mixed-salt solutions. Open symbols represent the literature data.

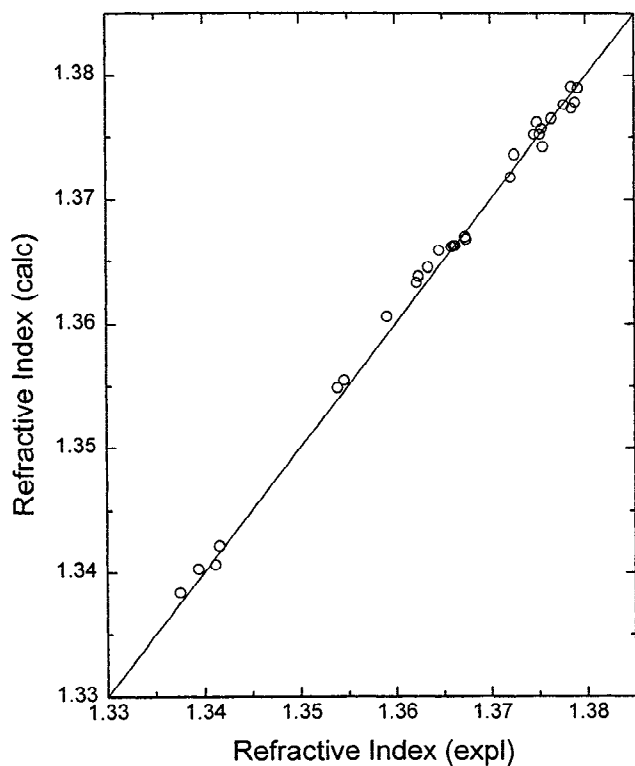


**Figure 9.** Comparison between experimental and predicted refractive indices of 27 mixed-salt solutions prepared in this study.

refraction method are plotted versus the measured values of the ternary solutions, using the measured solution densities and the partial ionic refraction data given in Table 2. The average error in refractive index value is 0.048%. It is clear that both the partial molal refraction and the density combination rule described above are excellent representations of the ternary solution data, at least for concentrations below saturation.

Light-scattering data obtained from droplet evaporation experiments provide the basis for deducing densities and refractive indices of mixed-salt solutions as a function of concentration, just as what was done with  $(\text{NH}_4)_2\text{SO}_4$  solution droplets described earlier. In addition, various density combination rules for mixtures may be further tested for high concentrations heretofore not accessible with bulk solutions. Figure 10a shows the light-scattering pattern observed with an evaporating solution droplet containing NaCl ( $x_2=0.291$ ) and  $\text{Na}_2\text{SO}_4$  ( $x_3=0.709$ ). Crystallization occurs at ~55% by weight of total solutes. Mie calculations with droplet densities given by equation (10) and partial molal refractions taken from Table 2 produce a scattering pattern, shown in Figure 10b, that matches the experimental observation almost point by point over the whole concentration range, as measured by the dc voltage changes during the evaporation experiment.

In Figure 11, densities predicted by various combination rules are compared with the values deduced from droplet evaporation as described above for the mixed-salt system  $\text{NaCl}-\text{Na}_2\text{SO}_4-\text{H}_2\text{O}$ . The densities of the binary solutions, shown as the two labeled outer curves, are computed from the polynomial expressions taken from Table 1. The dotted curve is the deduced solution densities for the mixture, using equation (10). If the solute mass fractions in equation (10) are replaced by the

corresponding mole fractions, the resulting densities are shown by the solid curve, which is distinctly different from the dotted curve, especially at high concentrations. The isopycnic method [Teng and Lenzi, 1975], which is the density analogue of the ZSR isopiestic relation, yields mixture densities in close agreement with those computed from equation (10), as can be seen by the solid symbols. On the other hand, the ionic strength molality fraction method [Teng and Lenzi, 1975], which assumes that the density of a mixed solution at a given ionic strength is additive in the densities (weighted by their molality fractions) of the individual binary solutions at the given ionic strength, yields mixture densities, shown by the open symbols, that are in good agreement with the dotted curve in low concentrations but gradually approach the solid curve at higher concentrations.

It is found that equation (10) applies equally well to the mixed-salt solution droplets containing  $\text{NaCl}-\text{NaNO}_3$ ,  $\text{NaCl}-\text{KCl}$ , or  $(\text{NH}_4)_2\text{SO}_4-\text{Na}_2\text{SO}_4$ . However, for  $\text{Na}_2\text{SO}_4-\text{NaNO}_3$ , best results were obtained for all compositions by using equation (10) in which the solute mass fractions were replaced by the corresponding mole fractions. Figure 12 shows that the light-scattering pattern produced by Mie computation with the mole-fraction based equation (10) for an evaporating  $\text{Na}_2\text{SO}_4$  ( $z_2=0.508$ ) -  $\text{NaNO}_3$  ( $z_3=0.492$ ) droplet is indeed in excellent agreement with the experimental observation.

### Light Scattering Properties

The thermodynamic and optical data obtained for the mixed-salt systems allow a definitive study to be made of the light-

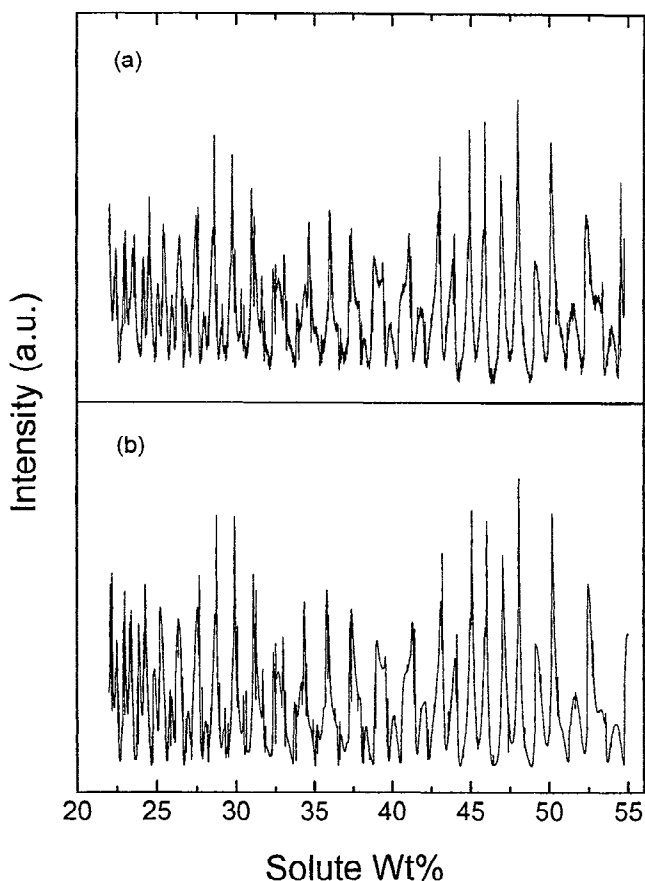


**Figure 10.** Light-scattering diagram of a mixed  $\text{NaCl}(x_2=0.291)-\text{Na}_2\text{SO}_4(x_3=0.709)$  solution droplet undergoing evaporation: (a) experimental observation and (b) computation.

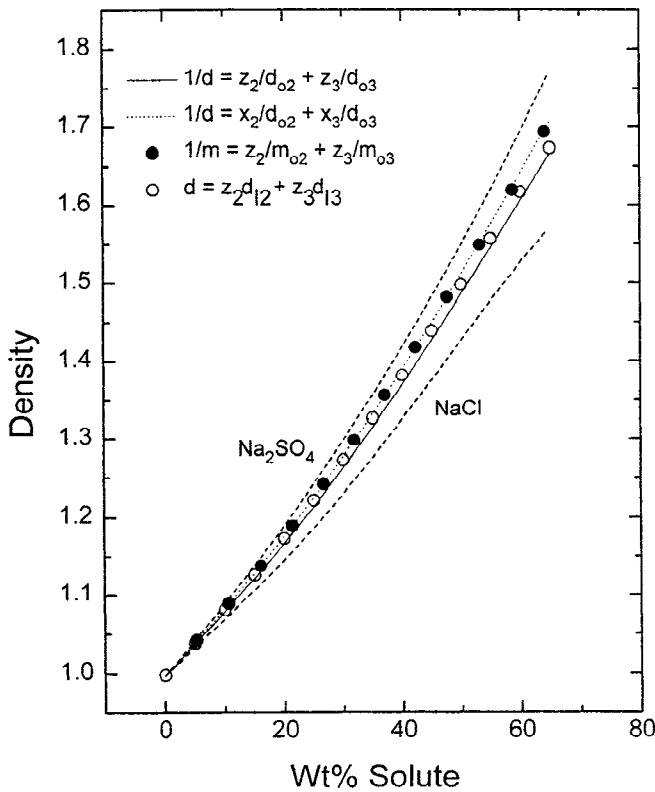


Figure 11. Comparison of density predictions by various combination rules with densities deduced from light-scattering data shown in Figure 10.

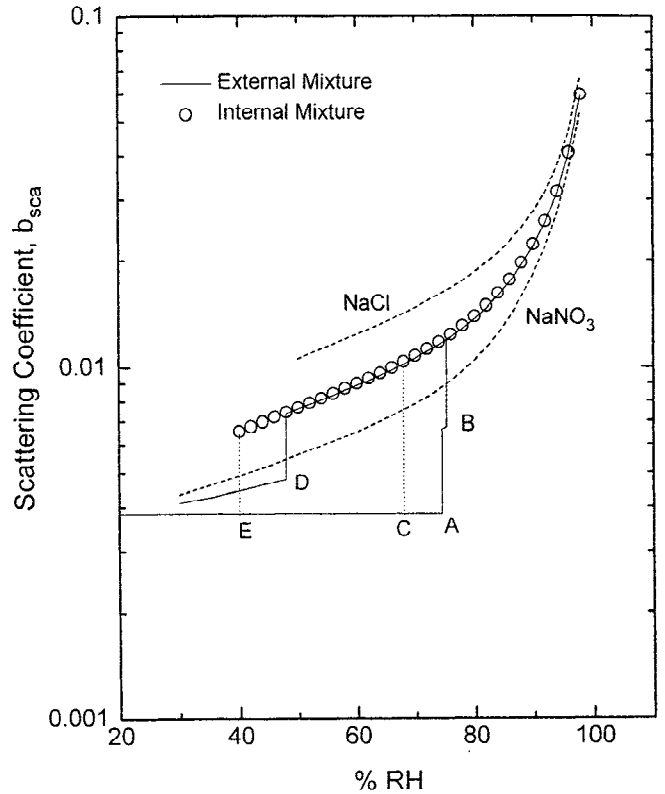


Figure 13. Humidity effect on scattering coefficients computed for internal and external mixtures of the mixed-salt aerosol: NaCl( $x_2=0.4$ )-NaNO<sub>3</sub>( $x_3=0.6$ ). The dry-salt particle size distribution is (0.3  $\mu\text{m}$ , 1.5) for both mixtures.

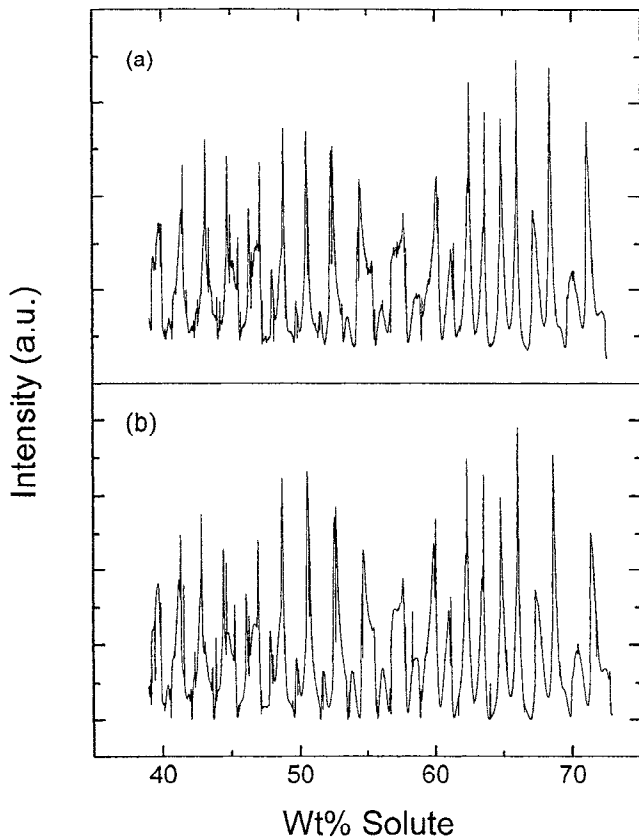


Figure 12. Light-scattering diagram of a mixed NaNO<sub>3</sub>( $z_2=0.492$ )-Na<sub>2</sub>SO<sub>4</sub>( $z_3=0.508$ ) solution droplet undergoing evaporation: (a) measurement and (b) computation.

scattering properties of external and internal mixtures composing the ambient aerosols. The method of computing aerosol scattering coefficients as a function of percent RH has been described elsewhere [Tang, 1996]. Briefly, the scattering coefficient  $b_{sca}$  for an aerosol of given size distribution  $f(D)$  with respect to diameter  $D$  may be computed, using the following formula:

$$b_{sca} = \int_0^{\infty} \pi(D/2)^2 Q_{sca}(\alpha, n) N f(D) dD \quad (11)$$

where  $\alpha$ , the optical parameter, is equal to  $\pi D/\lambda$ .  $N$  is particle number concentration, and  $Q_{sca}(\alpha, n)$  is single-particle scattering cross section for given  $\alpha$ , wavelength  $\lambda$ , and refractive index  $n$ . The wavelength,  $\lambda = 0.58 \mu\text{m}$ , is chosen as recommended by Presle and Horvath [1978] to give the maximum perception of an object under daylight conditions. At this wavelength, there is negligible absorption by either salts or their aqueous solutions, and therefore  $b_{sca}$  is equal to the extinction coefficient  $b_{ext}$ .

Throughout this study, a constant dry salt loading  $w_0$  of  $1 \mu\text{g m}^{-3}$  of air is employed as the basis of computation. Thus  $b_{sca}$  has the unit  $\text{km}^{-1} / (\mu\text{g m}^{-3})$ . The dry-salt particles are assumed to have a lognormal size distribution with count median diameter  $D_g$  and geometric standard deviation  $\sigma_g$ . The Kelvin effect due to droplet surface tension is neglected, and therefore percent RH is given by  $100a_w$ .

Figure 13 shows the humidity effect on the scattering coefficient of a mixed NaCl-NaNO<sub>3</sub> aerosol, the composition of which is 40-60 wt%, respectively. The dry-salt aerosol particles have a log-normal size distribution ( $D_g=0.3\mu\text{m}$ ;  $\sigma_g=1.5$ ). The

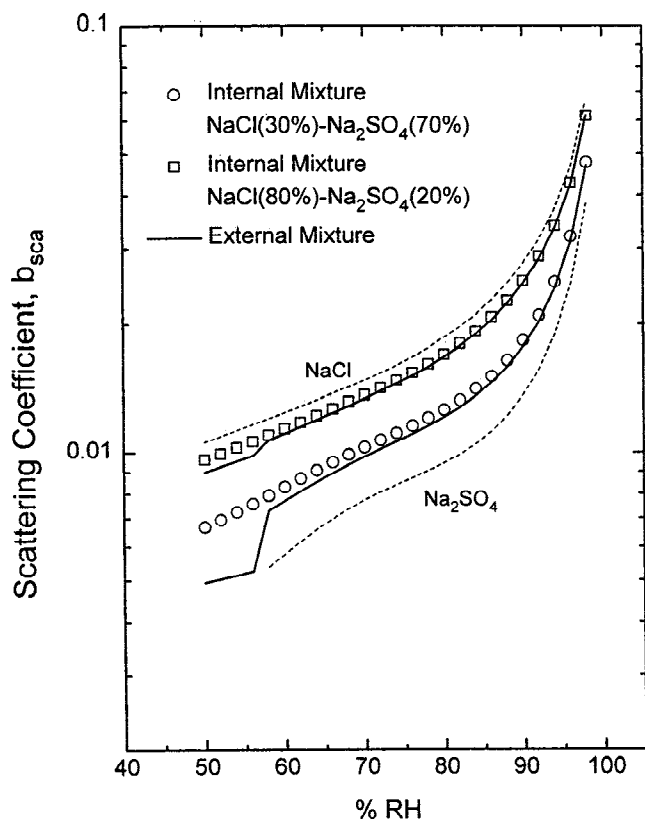


**Figure 14.** Humidity effect on scattering coefficients computed for internal and external mixtures of two mixed-salt aerosols: NaCl ( $x_2 = 0.3$ ) - Na<sub>2</sub>SO<sub>4</sub> ( $x_3=0.7$ ) and NaCl ( $x_2 = 0.8$ ) - Na<sub>2</sub>SO<sub>4</sub> ( $x_3=0.2$ ). The dry-salt particle size distribution is (0.3  $\mu\text{m}$ , 1.5) for all aerosols.

open symbols represent the behavior of the internally mixed droplets, whereas the solid curves represent the externally mixed droplets. The positions indicated by points A (74.5% RH) and B (75.3% RH) mark the deliquescence points of component aerosols NaNO<sub>3</sub> and NaCl, respectively, in the external mixture. Point C is the deliquescence point of the internally mixed aerosol. The NaCl droplets in the external mixture will crystallize out first at point D (~50% RH), whereas the NaNO<sub>3</sub> droplets will do so at much lower RH. In contrast, the internally mixed droplets will crystallize at point E (~40% RH). Thus the light-scattering properties of the internal and external mixtures as solution droplets are quite similar, but their phase transformation properties are different. The expected light-scattering behavior of the binary solution droplets are shown as the dashed curves, which enclose the mixed-salt aerosols as shown.

In Figure 14, the light-scattering properties of the mixed-salt solution aerosols, NaCl-Na<sub>2</sub>SO<sub>4</sub>, are shown as a function of percent RH for two different compositions. The open symbols represent the behavior of the internal mixtures, whereas the solid curves represent that of the external mixtures. Again, the two types of mixtures exhibit similar behavior if both have the same composition. In Figures 15 and 16, the light-scattering properties are shown for mixed-salt solution aerosols, NaNO<sub>3</sub>-Na<sub>2</sub>SO<sub>4</sub> and (NH<sub>4</sub>)<sub>2</sub>SO<sub>4</sub>-Na<sub>2</sub>SO<sub>4</sub>, respectively. The computations are performed for dry-salt aerosols with three different particle-size distributions, namely, (0.3  $\mu\text{m}$ , 1.5), (0.6  $\mu\text{m}$ , 1.5), and (0.6  $\mu\text{m}$ , 2.0). It is shown that for these sulfate and nitrate solution aerosols, the light-scattering properties do not

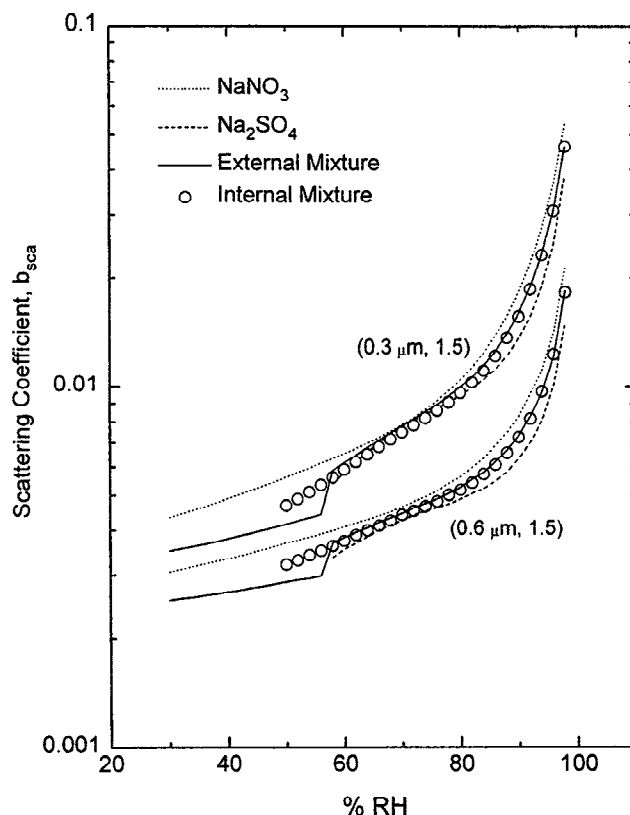


**Figure 15.** Humidity effect on scattering coefficients computed for internal and external mixtures of the mixed-salt aerosol: Na<sub>2</sub>SO<sub>4</sub> ( $x_2=0.487$ )-NaNO<sub>3</sub> ( $x_3=0.513$ ), for two dry-salt particle size distributions.

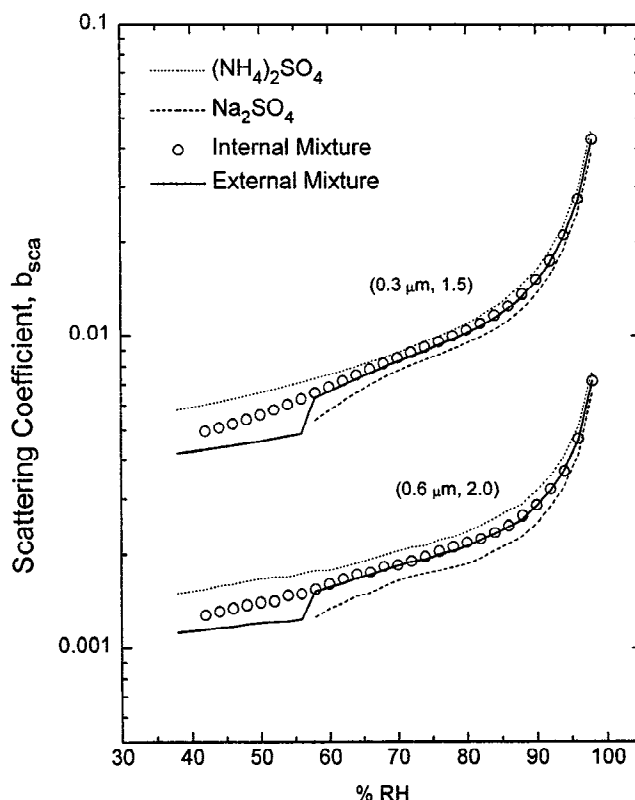


**Figure 16.** Humidity effect on scattering coefficients computed for internal and external mixtures of the mixed-salt aerosol: Na<sub>2</sub>SO<sub>4</sub> ( $x_2=0.5$ )-NaNO<sub>3</sub> ( $x_3=0.5$ ), for two dry-salt particle size distributions.

differ appreciably among all mixture types and compositions, as long as the dry-salt aerosols have the same particle-size distribution.

## Conclusions

Extensive water activity, density, and refractive index data at 25°C are presented for mixed-salt solutions, NaCl-KCl, NaCl-NaNO<sub>3</sub>, NaCl-Na<sub>2</sub>SO<sub>4</sub>, Na<sub>2</sub>SO<sub>4</sub>-NaNO<sub>3</sub>, and (NH<sub>4</sub>)<sub>2</sub>SO<sub>4</sub>-Na<sub>2</sub>SO<sub>4</sub>. The extended ZSR relation is found to be adequate for representing the water activity data for mixed-salt solutions over the entire concentration range from dilute solutions to high supersaturation. The simple volume additivity rule for mixed-salt solution densities is also acceptable in most cases investigated. In addition, partial ionic refractions are derived for all ions composing the solute molecules studied in this work. The extensive data obtained here have provided an opportunity to further explore the light-scattering properties of both internal and external mixtures of the chloride, sulfate, and nitrate aerosols of atmospheric importance. It is shown that for sulfate and nitrate aerosols as solution droplets, the light-scattering properties are similar for all mixture types and compositions, as long as the dry-salt aerosols have the same particle-size distribution. However, for mixed-salt aerosols containing NaCl, the light-scattering properties do depend upon both the composition and the particle-size distribution, although not so much on the mixture type. That NaCl stands out with H<sub>2</sub>SO<sub>4</sub> (not shown in the present work) as two efficient scatterers is due mostly to their ability to grow to larger sizes than other droplets under given humidity conditions [Tang, 1996]. Since NaCl is a major component of the sea-salt mixtures comprising the background aerosol in the marine atmosphere, the thermodynamic and optical properties of the mixed-salt aerosols containing NaCl are of particular importance. Work is forthcoming addressing the properties of sea-salt aerosols.

**Acknowledgments.** The author is indebted to his colleague, H. R. Munkelwitz, for the single-particle hydration measurements. The bulk solution measurements were made by Grace Hsueh of the University of Toronto during the 1995 summer appointment. This research was performed under the auspices of the U.S. Department of Energy under Contract No. DE-AC02-76CH00016.

## References

- Bezboruah, C. P., A. K. Covington, and R. A. Robinson, Excess Gibbs energies of aqueous mixtures of alkali metal chlorides and nitrates, *J. Chem. Thermodyn.*, **2**, 431-437, 1970.
- Bromley, L. A., Thermodynamic properties of strong electrolytes in aqueous solutions, *AIChE J.*, **19**, 313-320, 1973.
- Charlson, R. J., S. E. Schwartz, J. M. Hales, R. D. Cess, J. A. Coakley Jr., J. E. Hansen, and D. J. Hofmann, Climate forcing by anthropogenic aerosols, *Science*, **255**, 423-430, 1992.
- Clegg, S. L., and P. Brimblecombe, A generalized multicomponent thermodynamic model applied to the (NH<sub>4</sub>)<sub>2</sub>SO<sub>4</sub>-H<sub>2</sub>SO<sub>4</sub>-H<sub>2</sub>O system to high supersaturation and low relative humidity at 298.15 K, *J. Aerosol Sci.*, **26**, 19-38, 1995.
- Clegg, S. L., and K. S. Pitzer, Thermodynamics of multicomponent, miscible, ionic solutions: Generalized equations for symmetrical electrolytes, *J. Phys. Chem.*, **96**, 3513-3520, 1992.
- Clegg, S. L., K. S. Pitzer, and P. Brimblecombe, Thermodynamics of multicomponent, miscible, ionic solutions. 2. Mixtures including unsymmetrical electrolytes, *J. Phys. Chem.*, **96**, 9470-9479, 1992.
- Cohen, M. D., R. C. Flagan, and J. H. Seinfeld, Studies of concentrated electrolyte solutions using the electrodynamic balance. 1. Water activities for single electrolyte solutions, *J. Phys. Chem.*, **91**, 4563-4574, 1987.
- Fabuss, B. M., A. Korosi, and A. K. M. Shamsul Huq, Density of binary and ternary aqueous solutions of NaCl, Na<sub>2</sub>SO<sub>4</sub>, and MgSO<sub>4</sub> of sea waters and sea water concentrates, *J. Chem. Eng. Data*, **11**, 325-331, 1966.
- Hamer, W. J., and Y.-C. Wu, Osmotic coefficients and mean activity coefficients of uni-univalent electrolytes in water at 25°C, *J. Phys. Chem. Ref. Data*, **1**, 1047-1099, 1972.
- Kirgintsev, A. N., and A. V. Luk'yanov, *Isopiestic investigation of ternary solutions*, *Russ. J. Phys. Chem., Engl. Transl.*, **37**, 1501-1502, 1963.
- Kirgintsev, A. N., and A. V. Luk'yanov, *Isopiestic investigation of ternary solutions*, VIII, General treatment of the results for 34 ternary aqueous salt solutions, *Russ. J. Phys. Chem.*, **40**, 953-956, 1966.
- Larson, S. M., G. R. Cass, K. J. Hussey, and F. Luce, Verification of image processing based visibility models, *Environ. Sci. Technol.*, **22**, 629-637, 1988.
- Orr Jr., C., F. K. Hurd, and W. J. Corbett, (Aerosol size and relative humidity, *J. Colloid Sci.*, **13**, 472-482, 1958.
- Moelwyn-Hughes, E. A., *Physical Chemistry*, 2nd rev. ed., p. 397, Pergamon, Tarrytown, New York, 1961.
- Pitzer, K. S., and J. M. Simonson, Thermodynamics of multicomponent, miscible, ionic systems: Theory and equations, *J. Phys. Chem.*, **90**, 3005-3009, 1986.
- Platford, R. F., Isopiestic measurements on the system H<sub>2</sub>O-NaCl-Na<sub>2</sub>SO<sub>4</sub> at 25°C, *J. Chem. Eng. Data*, **13**, 46-48, 1968.
- Presle, G., and H. Horvath, Visibility in turbid media with colored illumination, *Atmos. Environ.*, **12**, 2455-2459, 1978.
- Robinson, R. A., Activity coefficients of sodium chloride and potassium chloride in mixed aqueous solutions at 25°C, *J. Phys. Chem.*, **65**, 662-667, 1961.
- Rood, M. J., M. A. Shaw, T. V. Larson, and D. S. Covert, Ubiquitous nature of ambient metastable aerosol, *Nature*, **337**, 537-539, 1989.
- Sanster, J., and F. Lenzi, On the choice of methods for the prediction of the water activity and activity coefficient for multicomponent aqueous solutions, *Can. J. Chem. Eng.*, **52**, 392-396, 1974.
- Sanster, J., T. T. Teng, and F. Lenzi, A general method of calculating the water activity of supersaturated aqueous solutions from ternary data, *Can. J. Chem.*, **51**, 2626-2631, 1973.
- Saxena, P., and T. W. Peterson, Thermodynamics of multicomponent electrolytic aerosols, *J. Colloid Interface Sci.*, **79**, 496-510, 1981.
- Seinfeld, J. H., Urban air pollution: State of science, *Scienc*, **243**, 745-752, 1989.
- Sloane, C. S., Optical properties of aerosols: Comparison of measurements with model calculations, *Atmos. Environ.*, **17**, 409-419, 1983.
- Sloane, C. S., and W. H. White, Visibility: An evolving issue, *Environ. Sci. Technol.*, **20**, 760-766, 1986.
- Stelson, A. W., Urban aerosol refractive index prediction by molar refraction approach, *Environ. Sci. Technol.*, **24**, 1676-1679, 1990.
- Stokes, R. H., and R. A. Robinson, Interactions in aqueous nonelectrolyte solutions, *J. Phys. Chem.*, **70**, 2126-2131, 1966.
- Tang, I. N., Phase transformation and growth of aerosol particles composed of mixed salts, *J. Aerosol Sci.*, **7**, 361-371, 1976.
- Tang, I. N., Deliquescence properties and particle size change of hygroscopic aerosols, in *Generation of Aerosols*, edited by K. Willeke, chap. 7, Butterworth-Heinemann, Newton, Mass., 1980.
- Tang, I. N., Chemical and size effects of hygroscopic aerosols on light scattering coefficients, *J. Geophys. Res.*, **101**, 19,245-19,250, 1996.
- Tang, I. N., and H. R. Munkelwitz, Simultaneous determination of refractive index and density of an evaporating aqueous solution droplet, *Aerosol Sci. Technol.*, **15**, 201-207, 1991.
- Tang, I. N., and H. R. Munkelwitz, Composition and temperature dependence of the deliquescence properties of hygroscopic aerosols, *Atmos. Environ.*, **27**, Part A, 467-473, 1993.
- Tang, I. N., and H. R. Munkelwitz, Water activities, densities and refractive indices of aqueous sulfates and sodium nitrate droplets of atmospheric importance, *J. Geophys. Res.*, **99**, 18,801-18,808, 1994a.
- Tang, I. N., and H. R. Munkelwitz, Aerosol phase transformation and growth in the atmosphere, *J. Appl. Meteor.*, **33**, 791-796, 1994b.
- Tang, I. N., H. R. Munkelwitz, and J. G. Davis, Aerosol growth studies, VI, Phase transformation of mixed salt aerosols in a moist atmosphere, *J. Aerosol Sci.*, **9**, 505-511, 1978.
- Tang, I. N., H. R. Munkelwitz, and N. Wang, Water activity measurements with single suspended droplets: The NaCl-H<sub>2</sub>O and KCl-H<sub>2</sub>O systems, *J. Colloid Interface Sci.*, **14**, 409-415, 1986.
- Tang, I. N., W. T. Wong, and H. R. Munkelwitz, The relative

- importance of atmospheric sulfates and nitrates in visibility reduction, *Atmos. Environ.*, *15*, 2463-2471, 1981.
- Teng, T.-T., and F. Lenzi, Water activity data representation of aqueous solutions at 25°C, *Can. J. Chem. Eng.*, *52*, 387-391, 1974.
- Teng, T.-T. and F. Lenzi, Density prediction of multicomponent aqueous solutions from binary data. *Can. J. Chem. Eng.* *53*, 673-676, 1975.
- Teng, T.-T., J. Sanster, and F. Lenzi, Additivity rules for the prediction of the density of aqueous solutions containing mixed-type solutes, *Can. J. Chem. Eng.*, *54*, 600-605, 1976.

Zdanovskii, A. B., *Tr. Solyanoi Lab. Vses. Inst. Galurgii Akad. Nauk SSSR*, no.6, 1936.

---

I. N. Tang, Environmental Chemistry, Department of Applied Science, Brookhaven National Laboratory, Upton, N. Y. 11973. (e-mail: intang@bnlarm.bnl.gov)

(Received March 13, 1996; revised August 15, 1996; accepted September 30, 1996.)